UJEAS

UNIZIK JOURNAL OF ENGINEERING AND APPLIED SCIENCES

UNIZIK Journal of Engineering and Applied Sciences 6(2), June (2026), 3466-3474
Journal homepage: https://journals.unizik.edu.ng/index.php/ujeas
PRINT ISSN: 2992-4383 || ONLINE ISSN: 2992-4391

Transient Simulation of a 240/120V Step Down Three-Phase to Five-Phase Transformer for Multiphase Drive Applications

Ifeanyichukwu Kalu Onwuka[1], Christopher Kalu Okoro[2], Miracle Tochukwu Uwakwe[3], Chukwuemeka Joseph Ejeagba[4], Marvelous Uchechi Ubani[5]
[1] Electrical and Electronic Engineering Department, Michael Okpara University of Agriculture Umudike, Nigeria.
[2] Electrical Electronic Engineering Technology Department, Dr. Ogbonnaya Onu Polytechnic Aba, Nigeria.
[3] Electrical and Computer Engineering Department, University of Connecticut, USA.
[4] Schneider Electric, Lagos, Nigeria.
[5]Electrical and Electronic Engineering Department, Michael Okpara University of Agriculture Umudike, Nigeria.
*Corresponding Author's E-mail: onwuka.ifeanyichukwu@mouau.edu.ng

Abstract
The increasing adoption of five-phase electrical machines in high-reliability and high-performance applications calls for efficient phase conversion from conventional three-phase utilities. Existing solutions predominantly rely on power electronic converters, which sadly introduce switching losses, electromagnetic interference, and increased system complexity. This paper builds on existing approach for developing a passive three-phase to five-phase transformer system with additional step-down functionality and electromagnetic validation. A generalized transformation matrix is derived to synthesize balanced five-phase voltages with 72° phase displacement from a 120° three-phase source. Winding turn relationships are formulated to integrate step-down voltage functionality without compromising phase symmetry. Magnetic circuit analysis by finite element analysis methods are used to evaluate flux distribution. Results demonstrate that balanced five-phase output stepped down from 240V to 120V can be achieved. The core loss obtained for the system is 2.87% with a symmetric flux distribution around the central limb and a flux density in the linear region of the B-H curve. The output voltage has a THD of 7.66%. These findings validate the proposed passive transformer system as a viable alternative for fixed-frequency multiphase applications requiring high reliability and galvanic isolation.

Keywords: Multi-phase transformer, five-phase system, finite element analysis, fixed-frequency, Multi-phase Drive Systems.

1. Introduction

The technology for multi-phase electric systems have matured in several applications, from generation to utilization. In particular, multi-phase drive systems have emerged as a superior alternative to conventional three-phase machines in applications requiring high reliability, improved torque-ampere characteristics, reduced torque ripple (Li *et al*., 2019), and green energy penetration (Tabrez *et al*, 2022). Five-phase machines offer excellent performance in safety-critical drives because they provide high fault-tolerant capability and improved torque performance compared with three-phase solutions, at the expense of a more complex machine model and control design (Li *et al*., 2019; Wei *et al*., 2022). Thus, five-phase systems offer a practical compromise between enhanced fault tolerance and manageable control complexity (Zhang *et al*., 2021).

A major challenge in the deployment of multi-phase systems is that conventional power supply is in three phases, necessitating an interface between the three-phase power supply and the multi-phase load. The interface between conventional three-phase infrastructure and multi-phase loads remains largely based on voltage source inverters, VSI (Chikondra *et al*., 2020). However, their ripple contents and frequencies of these ripples is a concern (Afonso *et al*, 2021). Also, there are noticeable inaccuracies when rotating machines are characterized using such systems (Kulandaival *et al*, 2023). Moreover, flexible inverter-based systems introduce switching losses and harmonics, EMI, and thermal constraints (Zhang *et al.*, 2024). This is a strong case for static converter systems from three phases to multi-phases, and transformers are very good candidates.

Traditional application of multi-phase transformer system is in rectifier systems to minimize harmonics and improve dc ripple characteristics (Abdollahi and Badfar, 2021). Tabrez *et al* (2022) provided important insights in the development of multi-phase transformers in general. For AC applications, researchers have developed three-phase to five-phase (Iqbal *et al*., 2010) and even three-phase to six-phase transformers (Iqbal and Singh, 2022). Most researchers on the subject focused on the connection topology and winding transformation for voltage magnitude balancing with 72^0 phase displacement in the output. Some of these researchers focused on the modeling and simulation of multiphase transformers using circuit-based tools such as MATLAB/Simulink (Sunil *et al.*, 2013; Bahrami and Gholamian, 2015; Dugglewar *et al.*, 2020; Bahadran and Keshavarz, 2023), providing useful insights to the application of these systems but lacking electromagnetic design validation. Others relied on the robust functionalities of the finite-element-analysis-based (FEA-based) ANSYS Maxwell for simulating and optimizing electromagnetic devices to model and simulate the three-phase to five-phase transformer (Khelafi *et al*., 2023; Nor *et al*., 2015; Karim *at al*., 2015; Brkic, 2023). This literature focused on 1:1 voltage ratios, and there is hardly any reported research on three-phase to five-phase step down transformers. While earlier works primarily relied on circuit-level and Simulink-based models, this paper presents a field-level finite-element model of a three-core shell-type, three – five-phase step-down transformer, enabling detailed evaluation of flux symmetry and core losses at the actual design voltage level.

The importance of this study for interoperable devices across nations with different distribution voltages is obvious.

2.0 Materials and methods

2.1 Subheading Sub-heading - second level heading.

2.1.1 Sub-subheading - third level heading.

2.1.1.1 Sub-sub-subheading fourth level heading.

Three identical shell-type cores were used for this study. Each phase of the three phases of the utility serves as the primary winding of the respective cores, identified as *x-core*, *y-core*, and *z-core*. Henceforth, properties or variables with subscripts as *x* or *y* or *z* refer to those of the members of these cores, respectively.

Voltage transformation method proposed by Iqbal *et al.* (2010) and Onwuka *et al.* (2026) is suitable for the 1:1 transformation ratio. However, it can be adapted for an arbitrary transformation ratio T_r as in equation (1).

$$T_m = \frac{2T_r}{\sqrt{3}} \begin{bmatrix} \sin 120 & 0 & 0 \\ 0 & \sin 12 & -\sin 48 \\ -\sin 24 & \sin 36 & 0 \\ -\sin 24 & 0 & \sin 36 \\ 0 & -\sin 48 & \sin 12 \end{bmatrix} \quad (1)$$

Where T_r is the ratio of the output to the input of the system. Hence the supply voltage on the primary winding is related to the output voltage by (2).

$$V_{5\,rms} = T_m V_{3\,rms} \quad (2)$$

With V_m being the peak voltage of the supply, and the $V_{5\,rms}$ and $V_{3\,rms}$ being the 5 by 1 and 3 by 1 output and input voltage vectors, respectively. The physical meaning of (1) is the turn ratio between the secondary and the primary windings of the indicated transformer cores. Equations (1) and (2) combined suggest the winding connection diagram of Figure 1.

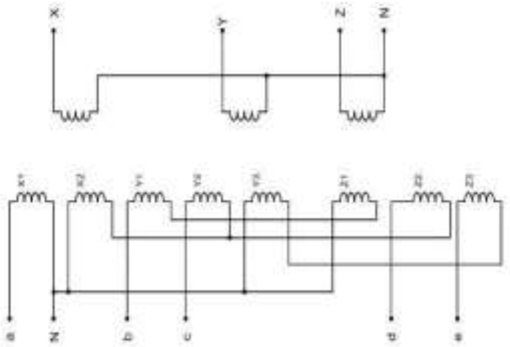

Figure 1. Winding Connection Diagram

The five-phase output and three-phase input voltage vectors are given by (3) and (4).

$$V_{5\ rms} = V_m \cos\left(\theta - \frac{2\pi m}{5}\right) \quad \text{for } m = 0, 1, 2, 3, 4. \tag{3}$$

$$V_{3\ rms} = V_m \cos\left(\theta - \frac{2\pi n}{3}\right) \quad \text{for } n = 0, 1, 2. \tag{4}$$

The core dimension is selected by first obtaining the cross-sectional area A_i of the core using (5). Afterwards, this value was used to select the nearest core size from standard tables.

$$A_i = \frac{E_t}{\sqrt{2}\pi f B_m} \tag{5}$$

In (5), E_t is the induced voltage per turn, f is the supply frequency, and B_m is the maximum flux density.

The number of turns N of each winding is determined from (6).

$$N = \frac{V}{E_t} \tag{6}$$

Where V is the expected induced voltage in that winding. The conductor cross-sectional areas a are selected from a standard wire gauge (SWG) chart such that:

$$a = \frac{I}{\delta} \tag{7}$$

Where I and δ are the conductor current and the current density respectively. Thus the winding data is presented in Table 1.

Table 1. Winding data

Coil	SWG	Voltage (V)
X,Y,Z	16	240
X1	17	120
X2	16	56.36
Y1=Z3	17	28.81
Y2=Z2	17	81.60
Y3=Z1	17	103.20

The AEDT 2020 R1 was the simulation tool. The transient magnetic solution type was used. The windings were modeled as lumped parameters, but defined in the winding properties as stranded with the predetermined number of turns. The core material was edited in its material properties to indicate that it is of laminated sheets and the lamination direction was set to the z-axis. A model depth was selected such that when the stacking factor K_i is applied to the predetermined A_i in (5), the B_m selected in Table 2 adjusted to about 1.42T which is still a pre-saturation value from the material B-H curve shown in Figure 2.

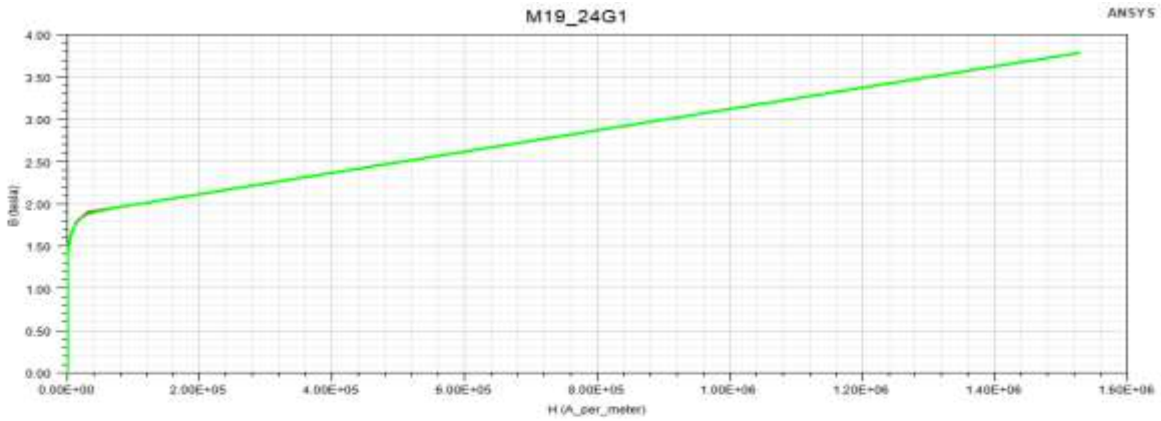

Figure 2. B-H Curve of M19-24G

M19_24G was selected as the electromagnetic material due to its low loss properties when compared to the commercial steel, steel_1008.

Table 2. Parameter values

S/N	Parameter	Value
1	E_t	1.2 V
2	B_m	1.35 T
3	δ	2.5 A/mm^2
4	*Q per core*	1 kVA
5	V_p / V_o	240/120V RMS
6	*Magnetic material type*	M19-24G
7	K_i *(Stacking factor)*	0.95
8	Core type/size	EL-180

In Table 2, a voltage per turn, flux and current densities are as recommended by Mittle and Mittal (2018). Furthermore, the length-based inside selection option was selected for the meshing operation and the maximum mesh size of 3mm and 0.7 mm selected for the cores and coils respectively. The mesh plot presented in Figure 3 was zoomed to show how fine the mesh sizes are. Also, the electrical Steel model of losses was selected. The transient-trasient link was enabled for the purpose of co-simulation with the simplorer twin builder. Hence, the winding connections described in Figure 1 was implemented as in Figure 4. The resistors connected to each winding represented each winding resistance and is necessary to ensure convergence. Other measuring instruments were selected from the component library and connected as shown in the figure 4. Gradual excitation of transformers proposed by some authors like Chang and Kuo (2021) was used to avoid inrush current. The setup was simulated for 0.25 seconds.

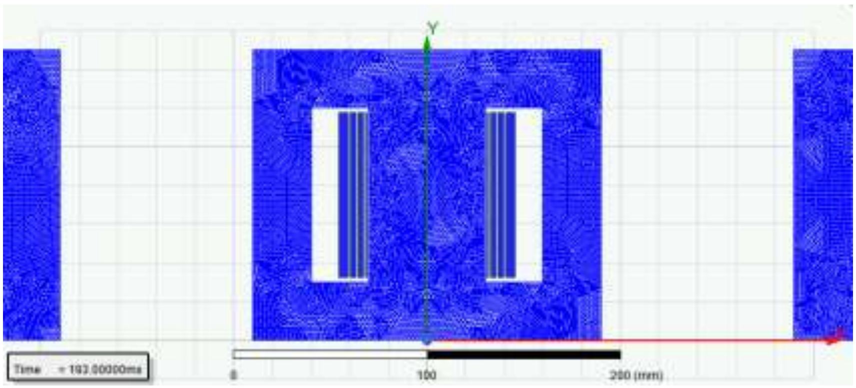

Figure 3. Mesh Plot of the Transformer

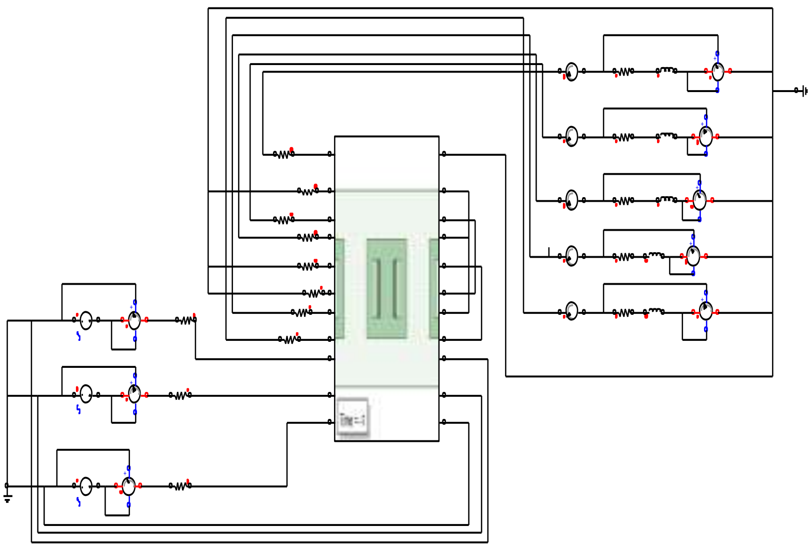

Figure 4. Maxwell/Twin-builder coupling

3.0 Result and Discussion

The three-phase excitation voltage and the five-phase output voltage are presented in figures 5 and 6 respectively. Figures 5 and 6 show that the 240/120 rms voltage transformation was achieved from the input to the output. Also, the output phase displacement is exactly 72^0 as required in a five-phase system.

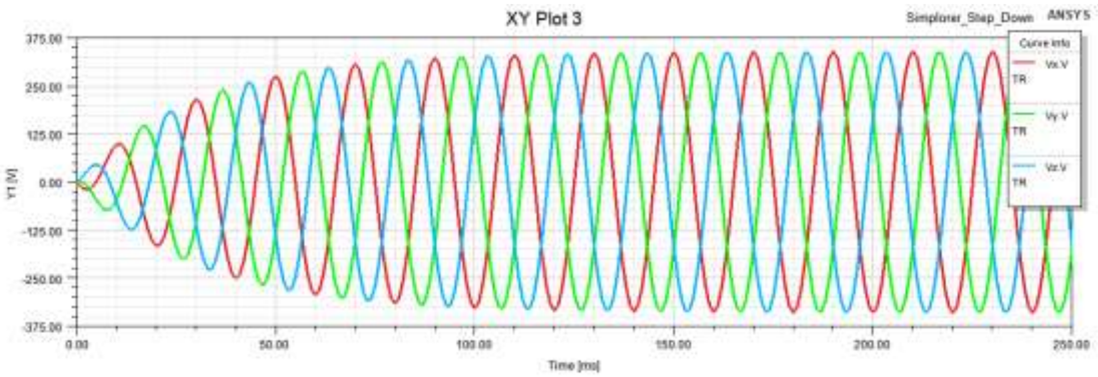

Figure 5. Three-phase input voltage

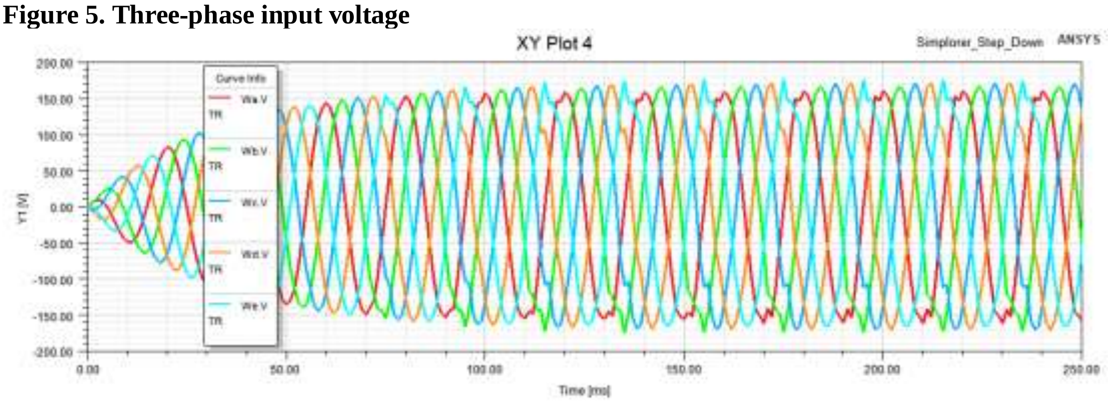

Figure 6. Five-phase output voltage

Figure 7 presents a simple analysis of the harmonics of the output voltage up to 500Hz, considered only for the steady-state (the last cycle of the simulation specifically). A THD of 7.66% was obtained, which is acceptable by regulations of both IEC 61000 series and IEEE 519 for grid connected supply systems. Although this result is inferior to the 4.6% obtained from an optimized system by Adam *et al.* (2024), it is noteworthy that this result has not been reported for multiphase step-down transformer to the best knowledge of the authors.

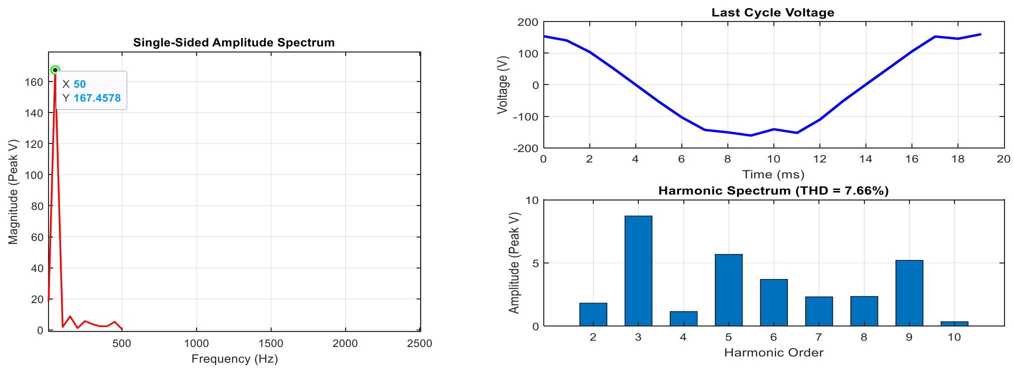

Figure 7: Output Voltage Harmonic Analysis: (a) Amplitude Spectrum; (b) Last cycle waveform and Harmonic Spectrum

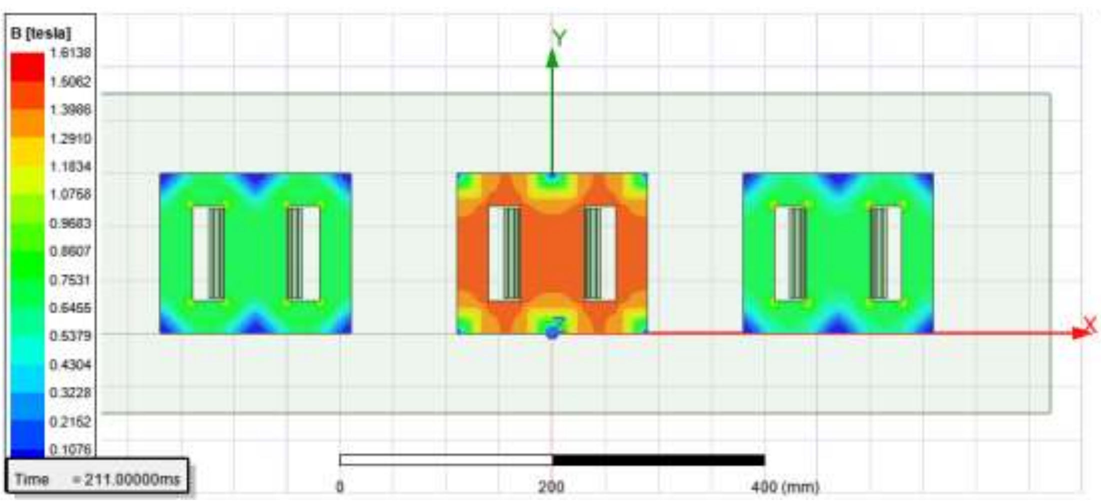

Figure 8. Flux density plot

The flux density observed at 0.211 seconds was plotted in Figure 8. The symmetry around the central limb is obvious and is similar to the results obtained by Bahadran and Keshavarz (2023), Brkic (2023), and Durmus and Mizrak (2024). The maximum flux density is within the range desired, more than 1.3T but less than 1.5T which implies that the transformer operates in the magnetic linear region (Durmus and Mizrak, 2024).

Another interesting observation is the core loss of the system of three cores, shown in Figure 9. This core loss is the sum of the hysteresis, eddy current, and excess losses of the three cores of the transformer. This approximates to 2.87% losses at the core for each of the three cores, which agrees with the known behaviour of M19_24G as a low loss electromagnetic material. The voltages induced in each of the windings of each of the three cores are captured in Figures 10 - 12. These results agree exactly with the rms values in Table 1.

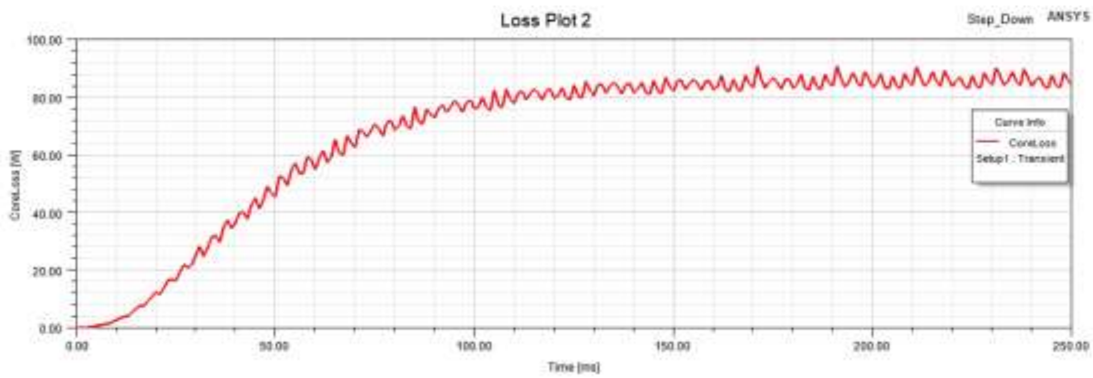

Figure 9. Plot of the Core Loss

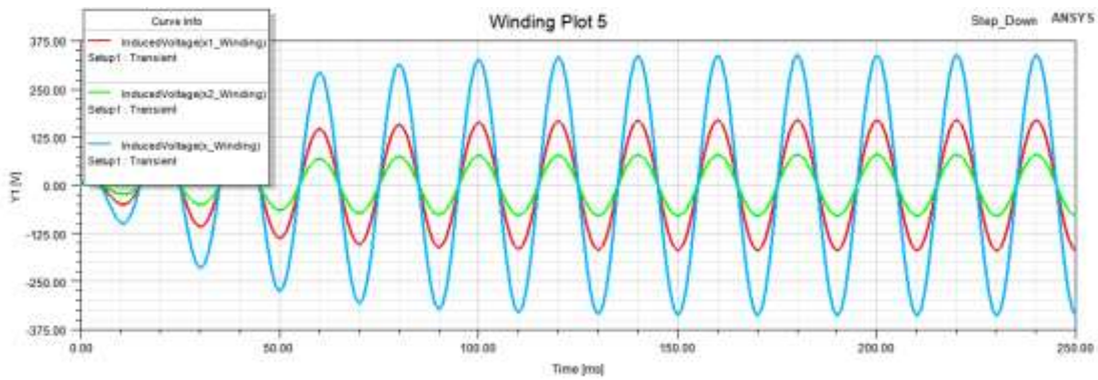

Figure 10. X-core voltages

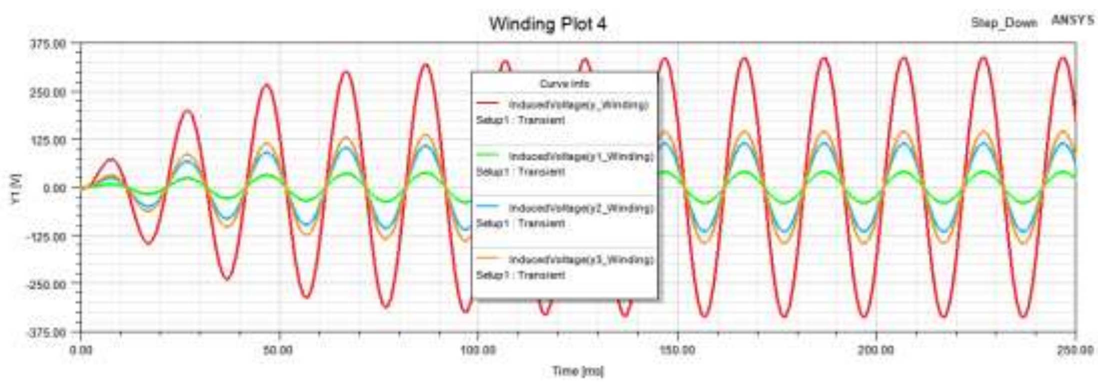

Figure 11. Y-core voltages

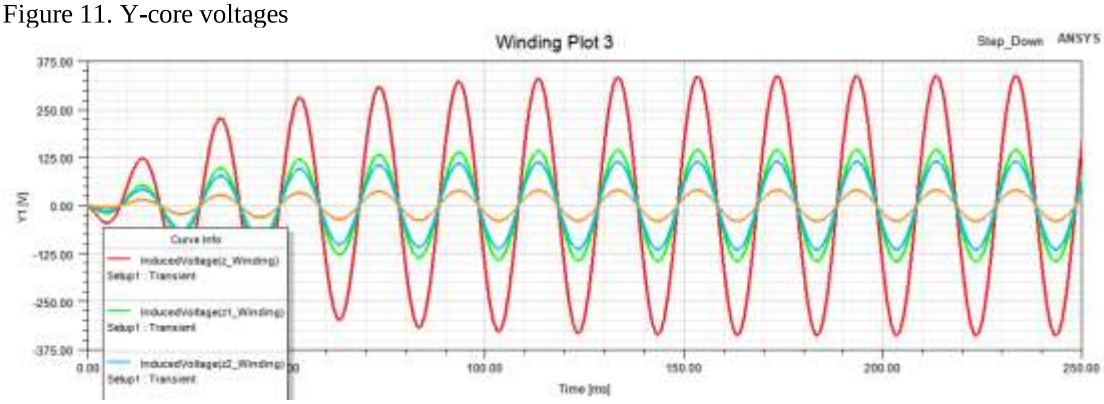

Figure 12. Z-core voltages

4.0. Conclusion

This study successfully demonstrated the viability of a passive three-phase to five-phase transformer system, providing a robust alternative to complex power electronic converters. The results confirm that the derived generalized transformation matrix and winding turn relationships accurately synthesize a balanced five-phase output with the required 72° phase displacement while achieving a precise 240V to 120V step-down functionality.

The finite element analysis (FEA) provided critical validation of the system's electromagnetic integrity. With a symmetric flux distribution and a low core loss of 2.87%, the transformer could operate efficiently within the linear region of the B-H curve, ensuring magnetic stability and high reliability. Furthermore, the inherent galvanic isolation provided by this passive approach makes it particularly suitable for high-performance applications where electromagnetic interference (EMI) must be minimized. While the system effectively achieves phase conversion, the recorded total harmonic distortion (THD) of 7.66% suggests an area for refinement.

5.0 Recommendation

Therefore, while the primary objectives of transformation and step-down functionality were met, further research is recommended to explore harmonic minimization techniques – such as optimized winding distributions or filtering – to further enhance the power quality for sensitive multiphase loads.

Acknowledgements

This research was sponsored by Tertiary Education Trust Fund.

References

Abdollahi, R., and Badfar, E., 2021. Harmonic mitigation approach by using pulse-doubling circuit in the AC-DC rectifier. *International Journal of Circuit Theory and Applications*, 49, 8, 2436 - 2452. https://doi.org/10.1002/cta.2991

Abdul Karim, K., Geok Yin, L., Mohd Yusoff, N. A., Othman, M. N., & Jidin, A., 2015. Design of five-phase transformer through finite element simulation. *Applied Mechanics and Materials*, 761, 12–16. https://doi.org/10.4028/www.scientific.net/amm.761.12

Adam, A., Kacar, F., and Uzunoglu C. P., 2024. Enhancement design of multi-phase transformer for cascaded H-bridge motor driver. *WSEAS Transactions on Circuits and Systems*, 23. DOI: 10.37394/23201.2024.23.17

Afonso, J. L., Tanta, M., Pinto, J. G. O., Monteiro, L. F. C., Machado, L., Sousa, T. J. C., and Monteiro, V. (2021). A Review on power electronics technologies for power quality improvement. *Energies*, 14, 24, 8585. https://doi.org/10.3390/en14248585

Bahadran A., and Keshavarz S. M., 2023. Investigating the three-phase to five-phase time converter using a special transformer connection. *Environmental Science and Geography*, 5, 2, e200531.

Bahrami M. and Gholamian S. M., 2015. Modeling and analysis of a three-phase to five-phase transformer, ResearchGate. [Online] Available: https://www.researchgate.net/publication/270552517_Modeling_and_Analysis_of_a_Three-Phase_to_Five-Phase_Transformer, accessed [10 January 2026].

Brkic, M., 2023. Numerical modeling and analysis of a single-phase transformer under the no-load condition. A Thesis submitted to the Faculty of Engineering, University of Ljubljana.

Chang, W.-C.; Kuo, C.-C. A. (2021). Novel excitation approach for power transformer simulation based on finite element analysis. *Appl. Sci.*, *11*, 10334. https://doi.org/ 10.3390/app112110334

Chikondra, B., Muduli, U., & Behera, R., 2020. Performance comparison of five-phase three-level NPC to five-phase two-level VSI. *IEEE Transactions on Industry Applications*, 56, 3767-3775. https://doi.org/10.1109/tia.2020.2988014.

Duggelwar V. S., Ahire M. R., Lonare S. N., Ghugarka M. A., and Shaik N. B., 2020. Review of analysis and spects of five-phase transformer by using MATLAB simulation, *International Research Journal of Engineering and Technology*, 7, 6, 4638 – 4642.

Durmus, F., and Mizrak, S., 2024. 115/230V 50Hz 2kVA step-up transformer on Ansys Maxwell. Downloaded from https://www.researchgate.net/publication/380397683_115230V_50HZ_2KVa_Step_Up_Transformer_on_ANSYS_MAXWELL [2 December 2025].

Iqbal A., Moinuddin S., Khan R. M., Ahmed S. M., and Abu-Rub H., 2010. A novel three-phase to five-phase transformation using a special transformer connection, *IEEE Transactions on Power Delivery*, 25, 3, 1637 – 1644.

Iqbal, A., and Singh, G.K., 2024. Three-phase to six-phase (asymmetrical double star) transformer. *IEEE Trans. Power Deliv.* 37, 5, 4481–4484. https://doi.org/10.1109/tpwrd.2022.3181847

Khelafi, A., Djebi, A., Touhami, O., Ibtiouen, R., 2023. Design and modeling of three-to-five phase three-limbed transformer. *IET Electr. Power Appl.* 17, 5, 670–686. https://doi.org/10.1049/elp2.12292

Kulandaivel G., Sundaram E., Gunasekaran M., and Chenniappan S., 2023. Five-phase induction motor drive-a comprehensive review. *Frontiers in Energy Research*. https://doi.org/10.3389/fenrg.2023.1178169

Li, G., Hu, J., Li, Y., & Zhu, J., 2019. An improved model predictive direct torque control strategy for reducing harmonic currents and torque ripples of five-phase permanent magnet synchronous motors. *IEEE Transactions on Industrial Electronics*, 66, 5820-5829. https://doi.org/10.1109/tie.2018.2870359.

Mittle, V. N. and Mittal, A., 2018. Design of electrical machines. *Standard Publishers Distributors*, New Delhi, India.

Nor A. M. Y., Kasrul A. K., Sharin A. G., Tole S., and Auzani J. (2015). Multiphase transforner modeling using finite element method, *International Journal of Power Electronics and Drive Systems*, 6, 1, 56 - 64.

Onwuka, I. K., Okoro, C. K., Ubani, M. U., Uwakwe M. T. and Ejeagba C., 2026. An optimized Three-phase to Five-Phase Transformer Winding Design. *Umudike Journal of Engineering and Technology*, 12, 1, 87 – 97. https://doi.org/10.33922/j.ujet_v12i1_10

Sunil K. J., Shalini J., Suresh Kumar P. G. V., and Wakijira F., 2013. Development of a three-phase to five-phase transformer using special techniques, *International Journal of Scientific and Engineering Research*, 4, 3.

Tabrez M., Sadhu P. K., Hossain Lipu M. S., Iqbal A., Husain M. A., and Ansari S., 2022. Power conversion techniques using multi-phase transformer: configuration, applications, issues and recommendations. *Machines*, 10, 13. https://doi.org/10.3390/ machines10010013

Wei, Y., Qiao, M., & Zhu, P., 2022. Fault-tolerant operation of five-phase permanent magnet synchronous motor with independent phase driving control. *CES Transactions on Electrical Machines and Systems*. https://doi.org/10.30941/cestems.2022.00014.

Zhang C, Jasni J, Mohd Radzi MA, Azis N and He X., 2024. Research and analysis of electromagnetic interference of a motor drive control system based on PMSM with SiC MOSFET for new energy electric vehicles. *Front. Energy Res.* 11:1338212. doi: 10.3389/fenrg.2023.1338212

Zhang, L., Zhu, X., Cui, R., & Han, S., 2021. A generalized open-circuit fault-tolerant control strategy for FOC and DTC of five-phase fault-tolerant permanent-magnet motor. *IEEE Transactions on Industrial Electronics*, 69, 7825-7836. https://doi.org/10.1109/tie.2021.3106012.